13th World Conference on Earthquake Engineering
Vancouver, B.C., Canada
August 1-6, 2004
Paper No. 1521

APPLICATION OF RESPONSE SPECTRUM METHOD TO PASSIVELY DAMPED DOME STRUCTURE WITH HIGH DAMPING AND HIGH FREQUENCY MODES

Yoji OOKI[1], Kazuhiko KASAI[2] and Shojiro MOTOYUI[3]

SUMMARY

This paper proposes use of viscoelastic (VE) dampers to a dome structure as one of possible passive control schemes for a space frame, and clarifies the relationship between the response characteristics and seismic input. The space frame with rectangular grids is adopted and VE dampers are installed. Good control performance is demonstrated via time-history analysis of a member-by-member model, using an accurate fractional derivative constitutive rule that simulates frequency-sensitivity of the dampers. For a detailed and mode-based analysis of the response characteristics, a so-called global damping model of the frame is also introduced. Effects of damping ratio and natural frequency of each mode are discussed by referring to the modal time histories and spectral responses. By the application of the dampers, the modes with high damping are obtained and they are in-phase with the applied earthquake. Those modes are combined adequately using the correlation coefficient which considers the characteristic of the earthquake.

INTRODUCTION

Arch, shell, or truss systems are usually applied to the space frames in practice. In these systems, the members supporting vertical loads should not be damaged because those members collapse abruptly if excessive stress arises. On the other hand, in the recent years, interest in enhancing seismic performance of the space frame has increased significantly, and much attention has been given to feasibility of using the base isolation and passive control schemes in Japan. When a system contained mode with high frequency, Gupta [1] showed that it is in-phase with the excitation, and proposed the effective modal combination method which combined CQC method [2, 3, 6, 7]. Kasai showed that synchronization of the modes were also observed in the case of highly damped systems [4], and extended Gupta's spectrum method using passively damped space frame model as the sample [5]. However, this technique requires dividing the response into rigid part and damper periodic part, and has left ambiguity. This paper applies CQC method using the correlation coefficient proposed by Der Kiureghian [6, 7], which can consider the characteristic of the earthquake, and show the comprehensive prediction method for maximum responses.

[1] Research Assoc., Tokyo Institute of Technology, Yokohama, Japan. Email: ooki@serc.titech.ac.jp
[2] Prof., Tokyo Institute of Technology, Yokohama, Japan. Email: kasai@serc.titech.ac.jp
[3] Assoc. Prof., Tokyo Institute of Technology, Yokohama, Japan. Email: motoyui@enveng.titech.ac.jp

CHARACTERISTICS OF SPACE FRAMES AND APPLICATION OF VE DAMPERS

Design and Dynamic Characteristics of Space Frame without Dampers

The study space frame consists of steel roof (space frame) and RC substructure, having plan dimension of 50 m x 50 m (Fig. 1). The roof has a rectangular grid pattern formed by a series of arches having rise span ratio 1/10. Arch member is a built-up curved girder of 1500 mm depth and made of identical upper and lower pipe members (ϕ276.4, t = 9.3 mm) connected by lacing members. Roof members and columns are designed against vertical load of 3626 N/m^2 (Dead Load 980 N/m^2 + Snow Load 2646 N/m^2). Lateral loads are supported by shear wall (10 x 8 x 0.15 m). Wind braces are placed at the perimeters of roof and they are designed against the wind load of 2195 N/m^2.

In the analysis, each girder is modeled by an equivalent beam element. Mass modeling is based on the followings: As for the roof, the reduced snow load of 0.35 x 2646 N/m^2 in addition to dead load is considered and the total is 1911 N/m^2. This is lumped to each node of roof structure. As for the RC substructure, a portion of mass ranging from 4 m to 8 m in height from the ground is lumped to the horizontal straight beam located at 8 m high from the ground. Remaining mass above the beam is lumped to the perimeter arches. Table 2 shows the periods, participation factors and effective mass ratios in the earthquake direction. 1st mode effective mass is only 45 % of the total mass and such a low effective mass ratio is rarely seen in regular buildings.

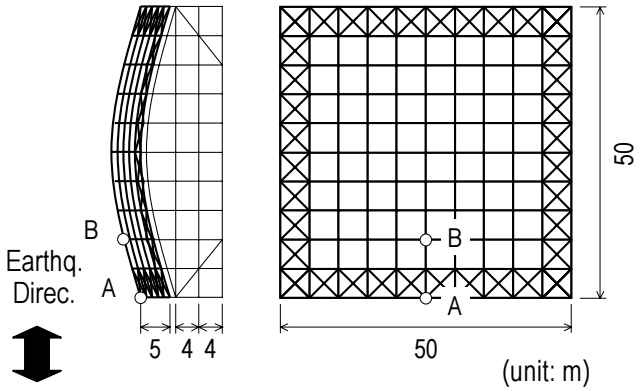

Figure 1. Space Frame and Substructure

Table 1. Members of Structure

Space Frame	Chord Member: ϕ276.4 t=9.3 mm Wind Brace: A=1800 mm^2 Young's Modulus: E=206 kN/mm^2 Allowable Stress: fc=196 N/mm^2, ft=235 N/mm^2
Substructure	Column: 1000x500 mm Beam: 500x250 mm Shear Wall: t=150 mm Young's Modulus: E=20.6 kN/mm^2 Allowable Stress: fc=15.7 N/mm^2

Table 2. Periods, Participation Factors and Effective Mass Ratios of System 1

Mode	Period (sec)	Participa -tion Factor $\beta_{n,x}$	Effective Mass Ratio (%)
1	0.529	0.706	45.1
2	0.529	-0.036	0.12
6	0.213	-0.049	0.22
7	0.213	0.225	4.59
8	0.202	0.240	5.20
9	0.202	-0.225	4.58
13	0.132	-0.257	5.99
14	0.132	0.178	2.86
18	0.116	-0.005	0.00
19	0.116	0.056	0.28
21	0.108	-0.251	5.70
22	0.108	-0.268	6.48

Application of VE Dampers and Models for Dynamic Analysis

The VE dampers are applied to the space frame and verified the efficiency using three space frame models (Fig. 2). System 1 is the original space frame mentioned before. System 2 is the space frame with wind braces in all roof grids. This type is often adopted in practice. System 3 has 20 VE dampers placed diagonally (VE Material: ISD111, Sumitomo 3M).

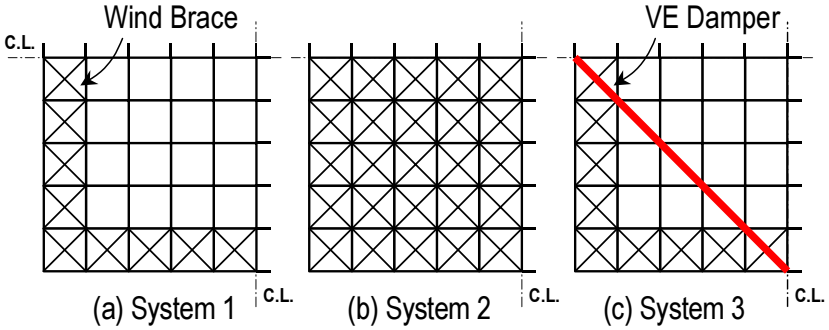

Figure 2. Studied Space Frames (1/4 Portion of Roof)

Since the rectangular grid has small in-plane stiffness, the deformations are efficiently introduced into the dampers under the earthquake. Arrangement of the dampers is determined in consideration of the 1st mode having the largest effective mass. Note that each damper is set identical, and thickness d = 8 mm and shear area A_s = 1.8 m^2, relatively small compared with the typical damper used for a regular building. The axial stiffness of the damper K_d' is designed to be equal to that of the wind brace having cross sectional area of 1800 mm^2 at the 1st period of System 1 (0.53 sec). The evaluation formula of VE material proposed by Kasai [8] is applied and Figure 4 shows the storage modulus G' and loss factor η of the material.

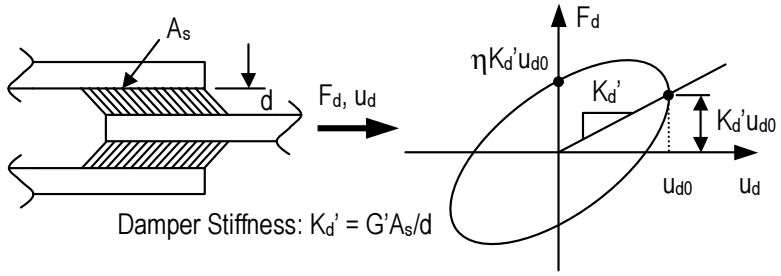

Figure 3. Viscoelastic Damper and Its Force-Deformation Curve

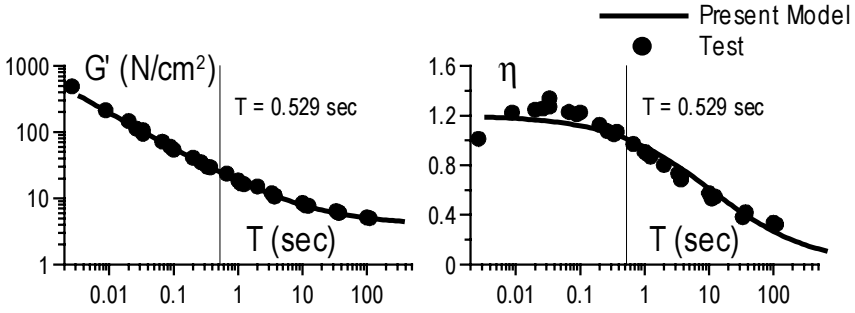

Figure 4. Frequency Sensitivities of Acrylic Viscoelastic Material

In dynamic analysis, Newmark-β (β = 0.25) numerical integration scheme with a time step Δt = 0.001 sec is used and Rayleigh damping is assigned to the space frame, so that the damping ratio is 0.02 at 1st (0.53 sec) and 13th (0.13 sec) modes. JMA Kobe earthquake record (1995, NS component, 0.84 g peak acceleration) and amplified El Centro (1940, NS, 0.52 g), Taft (1952, EW, 0.54 g) and Hachinohe (1968,

EW, 0.28 g) earthquake records are applied to these three space frames. The maximum velocity of amplified three earthquakes is set to 50 cm/s. In the following sections, mainly the results by JMA Kobe are shown. Studied frames are supposed to be linear system because geometrical nonlinearity of space frame hardly contributes to the response. Wind braces are ineffective under the compression load, so half of section area of the brace assumed to be effective.

3D-ANALYSIS OF SPACE FRAMES WITH OR WITHOUT VE DAMPERS

Figure 5 shows the responses of displacement and base shear. u_A and V are the displacement of node A and base shear parallel to the earthquake direction, respectively. w_B is the vertical displacement of node B (See Fig. 1). At these nodes, response displacement shows the maximum. The peak of u_A are 206, 95, 58 mm, w_B are 91, 45, 26 mm and V are 14229, 20134, 10787 kN in the order of System 1, 2 and 3. Accordingly, VE dampers have substantially reduced the responses. In System 2 and 3, response displacement is smaller than that of System 1, but response base shear is largest in System 2. System 3 shows the smallest response of the displacement and base shear.

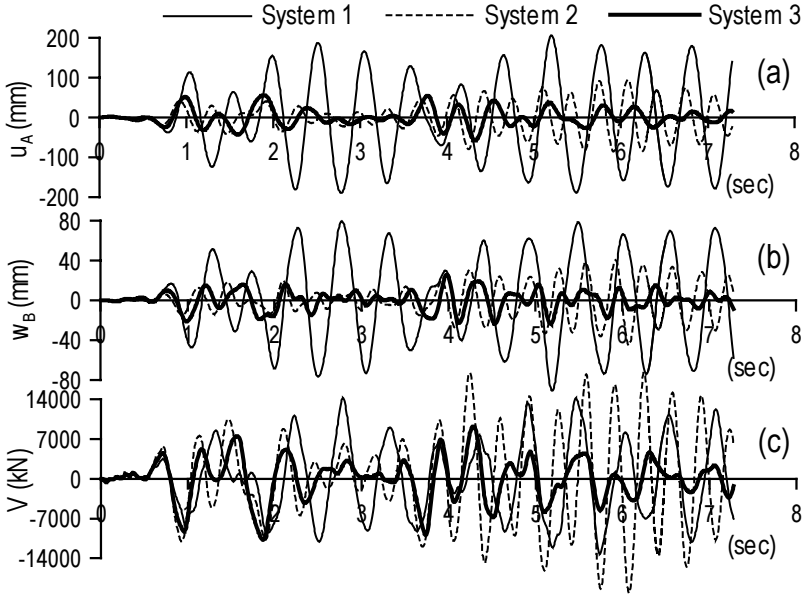

Figure 5. Response Time-History: (a) Displacement of Node A (Horizontal), (b) Displacement of Node B (Vertical) and (c) Base Shear

Figure 6 shows the damage of the roof members in three systems. In System 1 and 2, the stress exceeds the allowable stress in many arch and brace members. Contrary to it, in System 3, arch members are not damaged and the maximum ratio to the allowable stress of arch member is 0.52 under the JMA Kobe earthquake. Also, the maximum damper force and shear strain of VE material are 1084 kN, 166 %rad, respectively.

It is desirable not to damage the arch member supporting vertical load under a large earthquake and the performance of System 3 satisfies this requirement. The dampers in System 3 are installed according to the condition of deformation in the 1st mode and the mode shapes does not differ so much between the system with or without dampers. This application method of the damper is effective and the system shows better seismic performance compared with the case having only wind braces. These results are considered as the strict solution and used for evaluating the dynamic characteristics of System 3 in the following section.

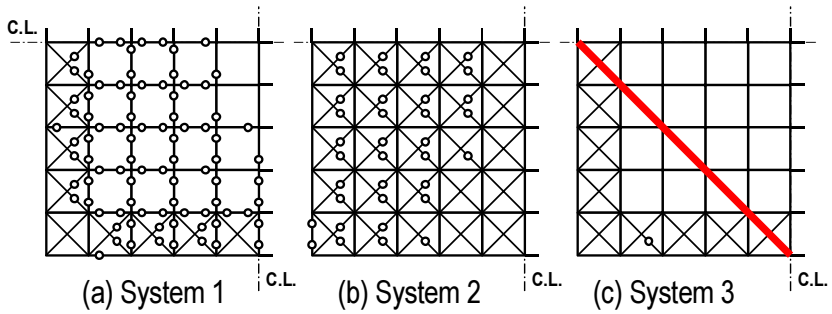

Figure 6. Damage of Space Frames under JMA Kobe (○: Stress is beyond allowable stress)

EVALUATION OF DYNAMIC CHARACTERISTICS USING GLOBAL DAMPING MODEL

Calculation Method of Mode, Period and Damping Ratio of Total System

If the modal analysis can be carried out, it is not only useful to analyze the dynamic characteristics of the system, also, possible to predict the maximum response of the system using the seismic response spectrum. However, System 3 is the non-proportional damping system and its stiffness and damping are changing with the frequency because of the frequency sensitivity of VE material. In order to avoid these complexities, the approximation technique of a global damping model is introduced. Eigenvalues and eigenvectors are obtained by the following iterative method: The stiffness matrix **K'** of total system including dampers has frequency dependency. Using the first mode circular frequency ω_1 of the System 1 (without dampers) as the initial estimate of ω_1, the axial stiffness of the damper corresponding to ω_1 (see Fig. 4) is obtained. Considering the stiffness of the damper, total stiffness is formed and Eq. (1) is solved.

$$\left[\mathbf{K}' - \{\omega_n\}^2 \mathbf{M} \right] \quad \boldsymbol{\phi}_n = \mathbf{0} \tag{1}$$

where **M** = mass matrix; $\boldsymbol{\phi}_n$ = n-th mode vector. Again ω_1 is obtained and only two or three iterations are required to reach the convergence. By naming the converged quantities as ω_1 and $\boldsymbol{\phi}_1$, the damping ratio h_n is calculated by using modal strain energy method.

$$h_n = \frac{\pi \sum_j \eta_{d,j}(\omega_1) K'_{d,j}(\omega_1) \{\Delta\phi_{n,j}\}^2}{2\pi \ \boldsymbol{\phi}_n{}^{\mathrm{T}} \mathbf{K}' \boldsymbol{\phi}_n} = \frac{\eta_d(\omega_1) K'_d(\omega_1) \sum_j \{\Delta\phi_{n,j}\}^2}{2\{\omega_n\}^2} \tag{2}$$

where η_d = loss factor; K_d' = axial stiffness for VE damper. Note that $\eta_d = \eta$; $K_d' = G'A_s/d$; $\Delta\phi_n$, j = modal axial deformation of j-th VE damper. Also the last expression of Eq. (2) assumes $\boldsymbol{\phi}_n{}^{\mathrm{T}}\mathbf{M}\boldsymbol{\phi}_n = 1$.
Table 3 shows the period, participation factor and damping ratio in the earthquake direction of System 3. Total damping ratio of n-th mode is sum of damping ratio of Eq. (2) and Rayleigh damping. Figure 7 shows 1st and 6th mode and vertical response is remarkable in 6th mode under the horizontal ground motion. In this case, axial deformation of VE damper becomes small and damping ratio of Eq. (2) shows small value accordingly.

Table 3. Periods, Participation Factors and Damping Factors of System 3

Mode	Period (sec)	Participa -tion Factor $\beta_{n,x}$	Damping Factor		
			Damper	Rayleigh	Total
1	0.400	-0.623	0.191	0.017	0.208
2	0.400	0.405	0.191	0.017	0.208
5	0.212	-0.019	0.002	0.016	0.018
6	0.212	0.273	0.002	0.016	0.018
9	0.157	0.205	0.151	0.018	0.170
10	0.157	0.279	0.151	0.018	0.170
16	0.115	0.142	0.010	0.022	0.031
17	0.115	0.061	0.010	0.022	0.031
18	0.109	0.226	0.098	0.023	0.120
19	0.109	-0.234	0.098	0.023	0.120
22	0.093	0.094	0.080	0.025	0.105
23	0.093	0.231	0.080	0.025	0.105

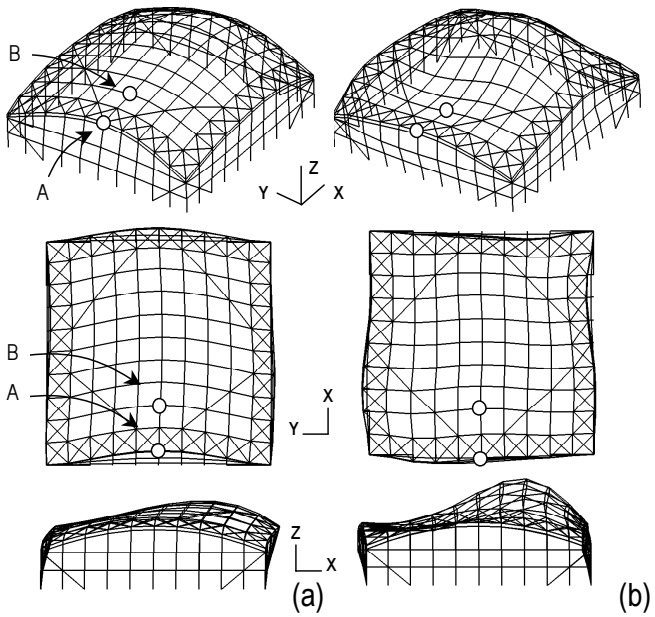

Figure 7. Vibration Modes of System 3: (a) 1st and (b) 6th Mode

Time-History Analysis Using Modal Superposition Method

The obtained modes are calculated based on the 1st mode frequency and it is required to verify the accuracy of the higher modes of the global damping model. Time-history analysis is performed using the modal superposition method and the result is compared with strict solution shown in section 3. Figure 8 shows the time-history of u_A, w_B and V of System 3. Dotted lines represent the strict solutions and the results of global damping model match well with them. In modal superposition method, from the 1st to 100th modes are considered and sum of the effective mass ratio of those modes is 96.5 %. Although proposed global damping model is obtained using the approximation method, sufficient accuracy is acquired.

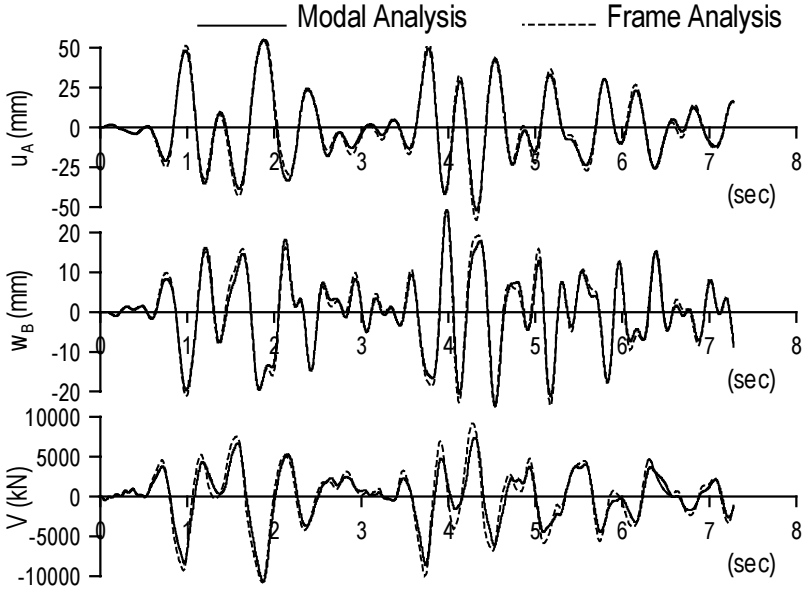

Figure 8. Comparison between Modal Analysis and Frame Analysis (JMA Kobe Earthquake)

EVALUATION OF RESPONSE OF SYSTEM 3

Evaluation Based on Response Time-History

Figure 9 shows the time-history responses of base shear of 1, 6, 10, 19 and 23rd mode and the period of each mode ranges from 0.40 to 0.09 sec. Damping ratios are about 10~20 % in these modes except for the 6th mode.

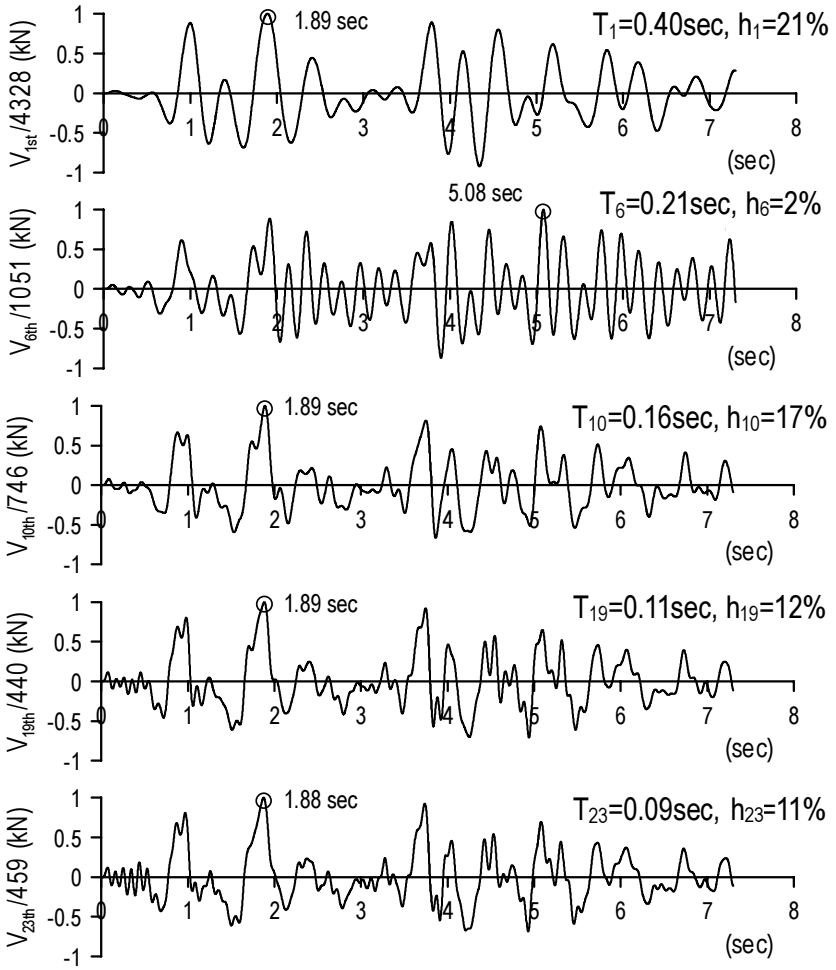

Figure 9. Response Time-History of Base Shear of 1st, 6th, 10th, 19th and 23rd Node (JMA Kobe)

The time-histories, except the 6th mode, are very similar, and produce the peak at the same time (1.9 sec). Since the mode having very short period shows the behavior like a rigid body, it is in-phase with a ground motion. In addition, the modes having high damping ratio oscillates in the same phase because the free vibration is decreased rapidly and a stationary response dominates. In this case, the high damping mode synchronizes with the earthquake motion regardless of the period. Only in the case of the 6th mode with low damping ratio (2 %), it considerably differs from the other 4 modes and it is based on the above reason.

The behavior of the modes with the very short period and high damping ratio is also observed in the case of the displacement response. However, since the 1st mode dominates in the response, the contributions are relatively small. These qualities are very important for the modal combination method explained later. In order to clarify the relationship between the response of the system and the ground motion, the analysis using the response spectrum is applied in the following section.

Evaluation Based on Response Spectrum

Figure 10 shows the pseudo-acceleration spectrum S_{pa} and displacement seismic response spectrum S_d of JMA Kobe and El Centro earthquake. The responses of the modes having significant effective mass in System 1 (without dampers) and System 3 (with VE dampers) are plotted.

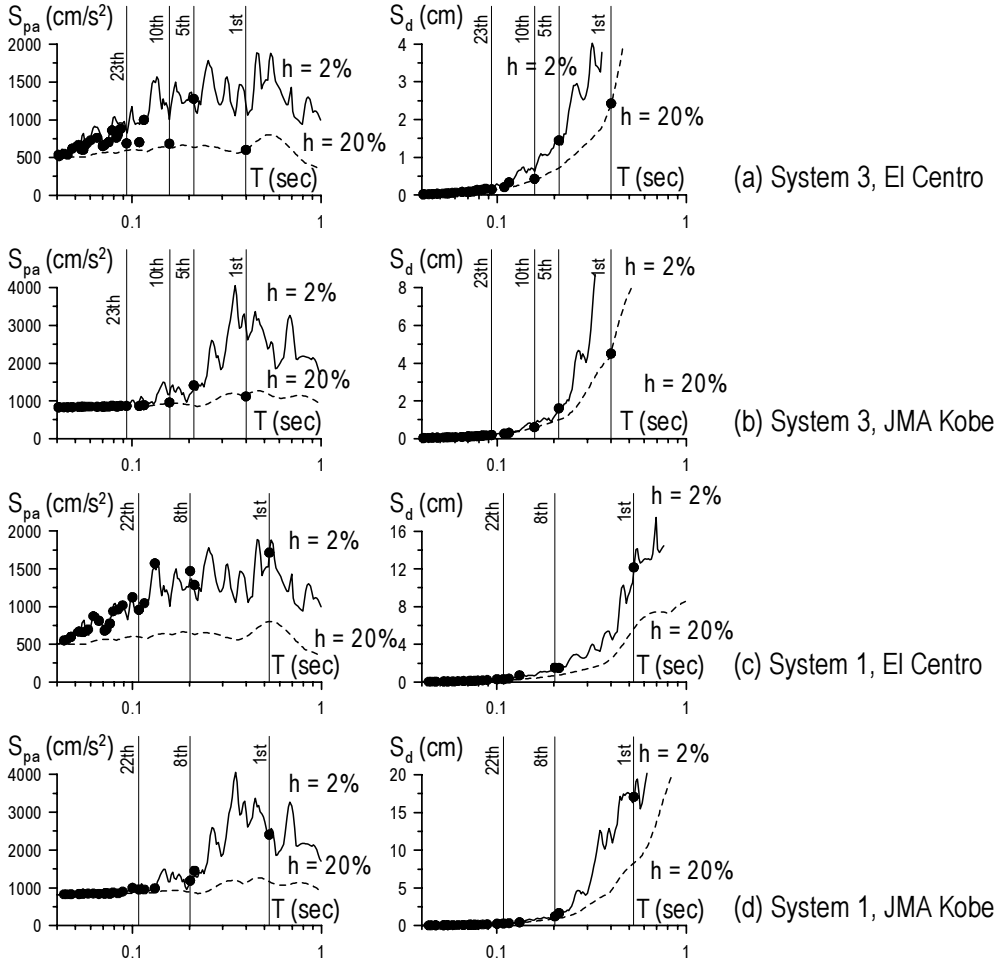

Figure 10. Pseudo Acceleration and Displacement Responses

As for the pseudo-acceleration, the response of System 1 gradually decreases as the period of the mode decreases and approaches the maximum earthquake acceleration. However, the damping ratio of System 3 varies considerably from mode to mode, and especially, the 6th mode has low damping ratio and show relatively large response. When the high order mode and high damping mode are in-phase with the ground motion, the acceleration response ratio to the maximum earthquake acceleration is almost equal to 1, and the modes show the rigid response. Many modes of System 1 and 3 exist in the rigid response domain (Fig. 10). On the other hand, as for the displacement response, the mode shows very small response under the short period domain regardless of the earthquake or magnitude of damping. The contribution of the 1st mode becomes larger compared to the case of base shear.

Prediction of Maximum Responses

Kasai [5] estimated maximum response according to the method proposed by Gupta [1], in which the response was classified into the rigid part and damped periodic part. However, it is generally difficult how to classify the rigid part and damped periodic part. On the other hand, Der Kiureghian introduced the CQC method [6, 7] and it combines the maximum responses of modes using the correlation

coefficient ρ_{ij}. Usually, ρ_{ij} is obtained by applying the white noise as the excitation, but Der Kiureghian also showed the formulation which uses the filtered white noise. In this case, the power spectrum density from the response of a single degree of freedom system against the white noise is used as a filtered white noise.

Maximum Response *Res* is evaluated by CQC method using the correlation coefficient ρ_{ij} between *i*-th and *j*-th mode. ρ_{ij} is obtained as follows;

$$Res^2 = \sum_i \sum_j \rho_{ij} Res_i Res_j \,, \quad \rho_{ij} = \frac{R_{ij}(0)}{\sqrt{R_{ii}(0)}\sqrt{R_{jj}(0)}} \tag{3a, b}$$

where Res_i = maximum response of i-th mode. $R_{ij}(0)$ is obtained by fourier inverse transform of cross spectrum $S_{ij}(\omega)$ between *i*-th and *j*-th mode (Eq. (4)), and ρ_{ij} in Eq. (3b) is shown as Eq. (5)

$$R_{ij}(0) = \frac{1}{2\pi}\int_{-\infty}^{\infty} S_{ij}(\omega)d\omega \tag{4}$$

$$\rho_{ij} = \int_{-\infty}^{\infty} S_{ij}(\omega)d\omega \Big/ \sqrt{\int_{-\infty}^{\infty} S_{ii}(\omega)d\omega} \Big/ \sqrt{\int_{-\infty}^{\infty} S_{jj}(\omega)d\omega} \tag{5}$$

$S_{ij}(\omega)$ is obtained from frequency response function $H(\omega)$ and power spectrum density of the earthquake G_F.

$$S_{ij}(\omega) = G_F(\omega)H_i^*(\omega)H_j(\omega) \tag{6}$$

$$H_i(\omega) = \frac{1}{\omega_i^2 - \omega^2 + 2h_i\omega_i\omega i} \tag{7}$$

$$G_F(\omega) = G_0 \frac{\omega_g^4 + 4h_g^2\omega_g^2\omega^2}{(\omega_g^2 - \omega^2)^2 + 4h_g^2\omega_g^2\omega^2} \tag{8}$$

Der Kiureghian applied Eq. (7) which simulates the characteristics of the earthquake. Usually, $G_F = G_0$ (white noise) is used in ordinary CQC method (CQC(WN) method). Substituting Eq. (7) and (8) for Eq. (6), power spectrum density of the earthquake is obtained and ρ_{ij} considering the characteristics of the earthquake is available for Eq. (3) (CQC(EQ) method). The detailed formula is shown in reference [7].

Four kinds of earthquakes, JMA Kobe (1995), El Centro (1940), Taft (1952) and Hachinohe (1968) are applied in this paper, and parameters of G_0, ω_g and h_g in Eq. (8) are determined in order to model these earthquakes. Table 4 shows ω_g and h_g for each earthquake, which are calculated using the least-squares method. G_0 is canceled out since it appears in the numerator and denominator of Eq. (5).

Table 4. ω_g and h_g for JMA Kobe, El Centro, Taft and Hachinohe

	ω_g/π	h_g
JMA Kobe (1995)	3.29	0.49
El Centro (1940)	3.54	0.51
Taft (1952)	4.94	0.51
Hachinohe (1968)	2.04	0.38

Correlation coefficients among typical five modes of System 3 and System 1 are shown in Table 5. The upper rows are the correlation coefficients obtained from the modal time-history, and those from CQC methods are shown on the lower rows. Kasai [5] pointed out that the correlation coefficients of CQC(WN) method show quite small value compared with those obtained from the modal time-history. If $G_F = G_0$ in Eq. (8), the characteristic of the excitation will be canceled out in Eq. (5) and no longer be taken at all into consideration in the correlation coefficient. Synchronization of the mode and excitation is not reproduced in this case. On the contrary, the correlation coefficients by CQC(EQ) method correspond comparatively well although the earthquakes are modeled simply by Eq. (8).

Table 5. Correlation Coefficient of CQC Methods

	1st	6th	10th	19th	23rd
1st	1.00	0.18 **0.04**	0.41 **0.11**	0.37 **0.04**	0.38 **0.02**
6th		1.00	0.29 **0.19**	0.19 **0.03**	0.20 **0.02**
10th			1.00	0.67 **0.36**	0.63 **0.19**
19th	System 3			1.00	0.90 **0.67**
23rd	El Centro				1.00

	1st	6th	10th	19th	23rd
1st	1.00	0.24 **0.04**	0.47 **0.11**	0.45 **0.04**	0.45 **0.02**
6th		1.00	0.67 **0.19**	0.63 **0.03**	0.63 **0.02**
10th			1.00	0.94 **0.36**	0.93 **0.19**
19th	System 3			1.00	0.98 **0.67**
23rd	JMA Kobe				1.00

(a) System 3, CQC(WN)

	1st	6th	10th	19th	23rd
1st	1.00	0.18 **0.19**	0.41 **0.47**	0.37 **0.43**	0.38 **0.43**
6th		1.00	0.29 **0.43**	0.19 **0.34**	0.20 **0.33**
10th			1.00	0.67 **0.79**	0.63 **0.74**
19th	System 3			1.00	0.90 **0.90**
23rd	El Centro				1.00

	1st	6th	10th	19th	23rd
1st	1.00	0.24 **0.20**	0.47 **0.49**	0.45 **0.46**	0.45 **0.45**
6th		1.00	0.67 **0.44**	0.63 **0.35**	0.63 **0.34**
10th			1.00	0.94 **0.79**	0.93 **0.74**
19th	System 3			1.00	0.98 **0.90**
23rd	JMA Kobe				1.00

(b) System 3, CQC(EQ)

	1st	7th	8th	13rd	22nd
1st	1.00	0.06 **0.00**	0.04 **0.00**	0.06 **0.00**	0.09 **0.00**
7th		1.00	0.21 **0.28**	0.07 **0.01**	0.12 **0.00**
8th			1.00	0.09 **0.01**	0.13 **0.00**
13rd	System 1			1.00	0.20 **0.04**
22nd	El Centro				1.00

	1st	7th	8th	13rd	22nd
1st	1.00	0.07 **0.00**	0.07 **0.00**	0.10 **0.00**	0.10 **0.00**
7th		1.00	0.66 **0.28**	0.49 **0.01**	0.49 **0.00**
8th			1.00	0.56 **0.01**	0.57 **0.00**
13rd	System 1			1.00	0.65 **0.04**
22nd	JMA Kobe				1.00

(c) System 1, CQC(WN)

	1st	7th	8th	13rd	22nd
1st	1.00	0.06 **0.04**	0.04 **0.04**	0.06 **0.06**	0.09 **0.07**
7th		1.00	0.21 **0.37**	0.07 **0.18**	0.12 **0.20**
8th			1.00	0.09 **0.19**	0.13 **0.21**
13rd	System 1			1.00	0.20 **0.31**
22nd	El Centro				1.00

	1st	7th	8th	13rd	22nd
1st	1.00	0.07 **0.05**	0.07 **0.05**	0.10 **0.07**	0.10 **0.08**
7th		1.00	0.66 **0.38**	0.49 **0.19**	0.49 **0.21**
8th			1.00	0.56 **0.19**	0.57 **0.22**
13rd	System 1			1.00	0.65 **0.31**
22nd	JMA Kobe				1.00

(d) System 1, CQC(EQ)

Table 6 shows the prediction of the maximum responses of System 1 and 3 under four kinds of earthquakes using three kinds of modal combination method of SRSS, CQC(WN) and CQC(EQ). In these analyses, the results considering the effective masses of 80 and 96% are shown and compared with those from time-history analyses of modal superposition method. The errors of base shear of System 3 are rather large in the case of SRSS and CQC(WN) because rigid response is not considered in these methods. On the contrary, CQC(EQ) shows good agreement with results from modal time-history. This indicates that Eq. (3) can serve as comprehensive formulization of modal combination method, which is even applicable to the system with high damping and high frequency modes.

Table 6. Prediction of Maximum Responses Using Three Kinds of Modal Combination Method (Ratio to Modal Time-History Analysis)

		System 3								System 1							
		JMA Kobe		El Centro		Taft		Hachinohe		JMA Kobe		El Centro		Taft		Hachinohe	
Effective Mass Ratio		80% ~23rd	96% ~100th	80% ~23rd	96% ~100th	80% ~23rd	96% ~100th	80% ~23rd	96% ~100th	80% ~21st	96% ~100th	80% ~21st	96% ~100th	80% ~21st	96% ~100th	80% ~21st	96% ~100th
u_A (mm)	Time History	55.3	55.0	29.0	29.8	37.1	37.1	20.2	20.2	206	206	141	141	111	111	69.2	69.2
	SRSS	0.77	0.78	0.80	0.78	0.76	0.76	0.78	0.78	1.00	1.00	1.04	1.04	1.02	1.02	0.97	0.97
	CQC(WN)	1.01	1.01	1.03	1.01	0.99	0.99	1.01	1.01	1.00	1.00	1.04	1.04	1.02	1.02	0.97	0.97
	CQC(EQ)	**1.07**	**1.00**	**1.02**	**1.00**	**0.99**	**0.99**	**1.00**	**1.00**	**1.00**	**1.00**	**1.04**	**1.04**	**1.03**	**1.03**	**0.97**	**0.97**
w_B (mm)	Time History	25.7	25.6	16.0	16.0	22.6	22.6	9.70	9.70	91.1	91.1	62.5	62.5	51.6	51.6	29.1	29.1
	SRSS	0.85	0.85	0.89	0.89	0.89	0.89	0.98	0.98	0.94	0.94	0.98	0.98	0.94	0.94	0.98	0.98
	CQC(WN)	1.04	1.04	1.02	1.02	0.98	0.98	1.12	1.12	0.95	0.95	0.98	0.98	0.95	0.95	0.98	0.98
	CQC(EQ)	**0.97**	**0.97**	**0.94**	**0.94**	**0.97**	**0.97**	**0.84**	**0.84**	**0.94**	**0.94**	**0.98**	**0.98**	**0.95**	**0.95**	**0.94**	**0.94**
V ($x10^3$ kN)	Time History	9.28	10.7	5.05	5.71	5.96	6.40	3.18	3.43	13.6	14.2	10.2	10.3	7.58	7.47	4.37	4.56
	SRSS	0.53	0.46	0.56	0.50	0.59	0.55	0.59	0.55	0.89	0.86	0.86	0.85	0.91	0.93	0.91	0.88
	CQC(WN)	0.74	0.65	0.80	0.72	0.80	0.75	0.82	0.77	0.90	0.87	0.88	0.88	0.96	0.98	0.94	0.90
	CQC(EQ)	**0.88**	**0.82**	**1.00**	**0.98**	**0.87**	**0.85**	**1.13**	**1.13**	**0.93**	**0.92**	**0.92**	**0.95**	**0.98**	**1.03**	**1.09**	**1.11**

CONCLUSIONS

(1) VE dampers were installed to the space frame taking advantage of the small in-plane shear stiffness of the rectangular grid, and the response of the system was substantially reduced. The possibility of the space frame system not to damage the arch frame even under the large earthquake was shown.

(2) The global damping system of System 3 with VE damper was discussed. Using this approximate model, the modal period and damping ratio of the system was obtained, and the accuracy of the global damping model was verified compared with the time-history analysis.

(3) From the result of modal time-history analysis, it was verified that the short period and high damping mode were in-phase with the ground motion and show the rigid response. Those modes are correlated strongly and especially have influence on the response of base shear. On the other hand, as for the displacement response, the influence of the 1st mode is significant.

(4) The maximum response was predicted using the CQC method. Especially, if the characteristics of the excitation are considered, the accuracy of the prediction becomes better since the synchronization of the modes and earthquake was taken into account. Based on the seismic response spectrum, the relationship between the dynamic characteristics of the space frame, applied earthquake and response of the system was clarified.

ACKNOWLEDGEMENT

The Ministry of Education, Science and Culture provided support for this study in the form of Grants-in-Aid for Young Scientists, Category (B) (Research Representative: Yoji Ooki). The authors gratefully acknowledge the support.

REFERENCES

1. Gupta, A.K. “Response Spectrum Method” CRC Press Inc., 1992.
2. Rosenblueth, E. and Elorduy, J. “Response of Linear Systems in Certain Transient Disturbances” Proceedings of Fourth World Conference on Earthquake Engineering, Santiago, Chile, 1969; A-1: 185-196.
3. Clough, R.W. and Penzien, J. ”Dynamics of Structures, Second Ed.” New York: McGraw-Hill Inc., 1993.
4. Kasai, K., Jagiasi, A. and Jeng, V. “Inelastic Vibration Phase Theory for Seismic Pounding Mitigation” Journal of Structural Engineering, 1996; 122(10): 1136-1146.
5. Kasai K., Motoyui S. and Ooki, Y. “A Study on Application of Viscoelastic Dampers to a Space Frame and Response Characteristics under Horizontal Ground Motions” Journal of Structural and Construction Engineering (Transactions of AIJ), 2002; 561: 641-648. (in Japanese)
6. Der Kiureghian, A. “On Response of Structures to Stationary Excitation” Report No. UCB/EERC-79/32, EERC, University of California, Berkeley, 1979.
7. Der Kiureghian, A. “A Response Spectrum Method for Random Vibration” Report No. UCB/EERC-85/15, EERC, University of California, Berkeley, 1980.
8. Kasai, K., Teramoto, M., Ookuma, K. and Tokoro, K. “Constitutive Rule for Viscoelastic Materials Considering Temperature, Frequency and Strain Sensitivities (Part1 Linear Model with Temperature and Frequency Sensitivities)” Journal of Structural and Construction Engineering (Transactions of AIJ), 2001; 543: 77-86. (in Japanese)
9. Ooki Y., Kasai K. and Motoyui S. “Steel Dome Structure with Viscoelastic Dampers for Seismic Damage Mitigation” Proceedings of the Conference on Behavior of Steel Structures in Seismic Areas, Naples, Italy, 2003; 641-648.